Incommensurate Sinusoidal Oxygen Modulations in Layered Manganites $La_{1-x}Sr_{1+x}MnO_4$ ($x \geq 0.5$)

Joaquín García,[1,*] Javier Herrero-Martín,[2] Gloria Subías,[1] Javier Blasco,[1] J. S. Andreu,[2] and M. Concepción Sánchez[1]
[1]*Instituto de Ciencia de Materiales de Aragón, CSIC- Universidad de Zaragoza, C/ Pedro Cerbuna 12, E-50009 Zaragoza, Spain*
[2]*Institut de Ciència de Materials de Barcelona- CSIC, Campus Universitari de Bellaterra, E-08193, Bellaterra, Barcelona, Spain*
(Received 11 July 2012; published 4 September 2012)

We have studied the incommensurate-ordered phase in overdoped $La_{0.4}Sr_{1.6}MnO_4$ by resonant x-ray diffraction at the Mn K edge. Weak resonant superlattice $(h \pm 0.2\ h \pm 0.2\ 0)$ and $(h \pm 0.4\ h \pm 0.4\ 0)$ reflections of the tetragonal structure were found below ~240 K. The energy, azimuth angle, and polarization dependencies of the resonant scattering have revealed sinusoidal modulations of the oxygen motions that are transverse and longitudinal to the tetragonal [110] direction. This result discards (Mn^{3+}, Mn^{4+})-like stripe-type order but point to a charge-density-modulation picture.

DOI: 10.1103/PhysRevLett.109.107202 PACS numbers: 75.25.Dk, 71.45.Lr, 75.47.Lx, 78.70.Ck

Manganites near half-doping show phase transitions traditionally associated with a charge-orbital ordering of Mn^{3+} and Mn^{4+} ions following a checkerboard pattern [1–3]. The $La_{0.5}Sr_{1.5}MnO_4$ layered perovskite has been long considered as the typical example of these charge-orbital-ordered manganites [4]. Recently, the charge difference between the two manganese sites (about 0.2 electrons) has been found to be much smaller than the one expected for a full ionic disproportionation [5–7], but the charge modulation has been still regarded as an ordered superlattice of electron poor (Mn^{4+}-like) and electron-rich (Mn^{3+}-like) ions. In a recent paper, we have shown, using the resonant x-ray scattering (RXS) technique, that the checkerboard ordering in $La_{0.5}Sr_{1.5}MnO_4$ is nicely explained as due to the condensation of three soft modes acting on the oxygen atoms [8]. The associated charge disproportionation, as well as the local anisotropy of the two different crystallographic Mn sites, results from these atomic displacements, discarding any kind of ionic charge-orbital ordering.

For overdoped compounds ($x > 1/2$), incommensurate charge ordering occurs with a wave vector that depends linearly on the extra charges as $2\varepsilon \approx (1 - x)a$, where a is the reciprocal-lattice vector. This fact has suggested the occurrence of a pattern of stripes as several models claimed [3,9–14]. Alternatively, a charge-orbital density wave of e_g electrons has also been proposed by x-ray and neutron diffraction measurements as well as transmission electron microscopy [15–21]. Thus far, the precise nature of the charge and lattice modulation for overdoped manganites is still unknown.

In this Letter, we have investigated the insulating phase of the overdoped $La_{0.4}Sr_{1.6}MnO_4$ manganite. This compound exhibits an incommensurate superstructure below $T \sim 240$ K, which has been also related to the ordering of charge and orbitals of e_g electrons as in $La_{0.5}Sr_{1.5}MnO_4$. We have made use of the atomic selectivity of the RXS technique at the Mn K edge to determine the charge and lattice modulations of the Mn sublattice by analyzing the energy, azimuth angle (φ), and polarization dependences of the observed superlattice reflections. Here, we show that the incommensurate superstructural order in $La_{0.4}Sr_{1.6}MnO_4$ ($x = 0.6$) is characterized by the appearance of weak resonant superlattice $(h \pm \varepsilon\ h \pm \varepsilon\ 0)_t$ and $(h \pm 2\varepsilon\ h \pm 2\varepsilon\ 0)_t$ reflections with a modulation vector of $2\varepsilon = 1 - x = 0.4$ (the subscript t indicates the room-temperature tetragonal unit cell). They correspond to the $(h \pm 1/4\ h \pm 1/4\ 0)_t$ and $(h \pm 1/2\ h \pm 1/2\ 0)_t$ commensurate modulations observed in $La_{0.5}Sr_{1.5}MnO_4$ ($2\varepsilon = 0.5$). The observed energy, azimuth angle, and polarization dependences of the resonant scattering at $(h \pm 0.2\ h \pm 0.2\ 0)_t$ and $(h \pm 0.4\ h \pm 0.4\ 0)_t$ reflections are well explained by the presence of two types of sinusoidal modulations of the oxygen displacements, transverse and longitudinal to the tetragonal [1 1 0] direction, respectively. Similar to the half-doped compound [8], we discard any bimodal (Mn^{3+}, Mn^{4+})-like ordering in stripes for the overdoped manganites.

$La_{0.4}Sr_{1.6}MnO_4$ single crystal was grown using a floating-zone furnace with oxygen pressure of 2 bars. The growth speed ranged between 12 and 10 mm per hour [22]. The sample was single phase with a tetragonal structure (space group $I4/mmm$, $a = 3.852$ Å and $c = 12.4$ Å) at room-temperature. The single crystal was cut and polished in the $(110)_t$ plane. RXS experiments at the Mn K edge were performed at the ID20 beam line [23] in ESRF (Grenoble, France). The incident monochromatic beam was linearly polarized (99%) perpendicular to the scattering plane (energy resolution being 1 eV). A four-circle vertical diffractometer was used equipped with a Cu (220) crystal analyzer for σ-σ' and σ-π' polarization measurements. The energy dependence spectra across the Mn K absorption edge were corrected for absorption by using the experimental fluorescence. Azimuth scans at the resonance energy were measured by rotating the sample around $\mathbf{Q}$, $\phi = 0°$ for $\boldsymbol{\sigma}$ polarization vector parallel to $[\bar{1}10]_t$. In order to get a reliable comparison between the experimental intensities and the theoretical simulations, we first estimated the

intensity ratio of the measured scattered intensities of both, $(h \pm 0.2\ h \pm 0.2\ 0)_t$ and $(h \pm 0.4\ h \pm 0.4\ 0)_t$ superlattice reflections, here studied by comparison to Thomson intense Bragg reflections within a relative error of about 30%. We chose the $(220)_t$ Bragg reflection and we normalized its experimental scattered intensity at energies far from the Mn K absorption edge to the square of the nonresonant structure factor in absolute squared electron units calculated with FDMNES [24] in the orthorhombic unit cell defined as $\mathbf{a}_o = \mathbf{a}_t + \mathbf{b}_t$, $\mathbf{b}_o = \mathbf{a}_t - \mathbf{b}_t$, $\mathbf{c}_o = \mathbf{c}_t$. (From here on the $\sqrt{2}\mathbf{a}_t \times \sqrt{2}\mathbf{a}_t \times \mathbf{c}_t$ cell is used.) Finally, we expressed the intensity of the two types of superlattice reflections in absolute squared electron units by scaling to their respective experimental intensity ratios to the $(220)_t$. Since the crystal is a and b twinned, the intensity of the $(220)_t$ reflection has contributions of the two domains, whereas only one domain contributes to the superlattice reflections. We have also taken into account this fact in the normalization procedure assuming a 50-50 population.

The energy dependences of the $(1.6\ 1.6\ 0)_t$ and $(1.4\ 1.4\ 0)_t$ reflections recorded in the σ-σ' polarization channel at different φ angles are shown in Fig. 1(a). The two superlattice reflections, associated with the so-called charge ordering, have a similar energy dependence and resemble the behavior of the $(3/2\ 3/2\ 0)_t$ superlattice reflection in the $x = 0.5$ sample [8]. We observe the scattered intensity at energies below the Mn K edge, which comes from the atomic displacements breaking the $I4/mmm$ symmetry (Thomson scattering) and a broad main resonance with a strong intensity enhancement at 6556 eV, approximately 3 eV beyond the Mn K edge. This enhancement comes from the difference between the anomalous atomic scattering factors of Mn atoms located in different crystallographic sites. The spectral shape and the overall intensity of the $(1.6\ 1.6\ 0)_t$ reflection show a moderate azimuthal dependence as depicted in Fig. 1(a).

Figure 1(b) shows the energy dependences of the $(1 \pm 0.2\ 1 \pm 0.2\ 0)_t$ and $(2 \pm 0.2\ 2 \pm 0.2\ 0)_t$ reflections in the σ-π' channel. These reflections are ascribed to the so-called orbital ordering. No scattered intensity was observed at energies below the absorption edge but a strong resonance peak is visible at the energy of the Mn K edge. A polarization analysis indicates that the resonant scattering is purely π' polarized. The lack of a σ-σ' signal demonstrates that these reflections are forbidden by symmetry and they shall be classified as anisotropy of the tensor susceptibility (ATS) reflections [25,26]. The azimuthal dependence follows a π periodicity [see inset of Fig. 1(b)]. Intensities at different $\mathbf{Q}$ scattering vectors follow the $\cos^2\theta$ dependence. RXS spectra for these ATS reflections are strikingly reminiscent of those reported for $(h/4\ h/4\ 0)_t$-type reflections (h odd) in $La_{0.5}Sr_{1.5}MnO_4$, which suggests the presence of similar distortions of the MnO_6 octahedron [8].

The energy, polarization, and azimuthal behavior of the two types of reflections exhibit completely different

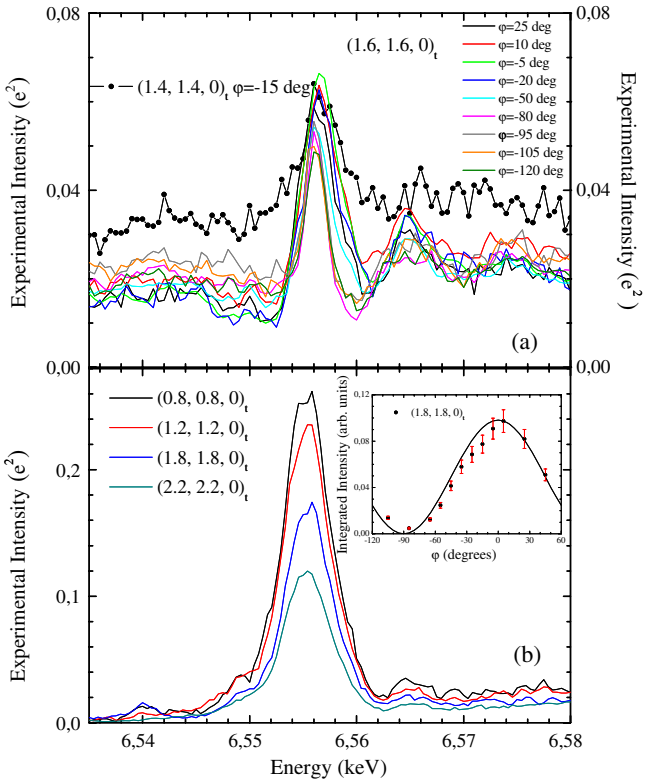

FIG. 1 (color online). Energy dependence around the Mn K edge of scattered intensities for $La_{0.4}Sr_{1.6}MnO_4$ at 80 K of (a) superlattice reflections collected in the σ-σ' polarization channel at different values of φ and (b) ATS reflections collected in the σ-π' polarization channel at $\varphi = 0°$. The inset shows the azimuthal angle dependence of $(1.8\ 1.8\ 0)_t$ intensity at the resonant peak, $E = 6.555$ keV (open circles). The solid line is the calculated intensity $\propto A\cos^2\varphi$.

characteristics from each other. However, for a bimodal distribution of Mn^{3+}- and Mn^{4+}-like atoms, all of the previous incommensurate reflections would show nonzero σ-σ' and σ-π' scattered intensity. The bimodal stripelike model cannot then explain either the lack of σ-σ' intensity in the $(h \pm 0.2\ h \pm 0.2\ 0)_t$ reflections or the intensity ratio between the observed superlattice reflections. Therefore, RXS data rule out any kind of bimodal Mn^{3+}- and Mn^{4+}-like ion ordering in $La_{0.4}Sr_{1.6}MnO_4$ and rather, they indicate the presence of a sinusoidal modulation of the anomalous atomic scattering factor of the Mn atoms. The terms of the Mn anomalous atomic scattering tensor (AAST) will be given by $f_{ij,n} = f_{ij,0} + \Delta f_{ij}\cos(2\pi\mathbf{q}\cdot\mathbf{r}_n + \alpha)$ with $\mathbf{q}$ the wave modulation vector, $\mathbf{r}_n$ the position of the n Mn atom, and α the phase. The anomalous structure factor tensor for this type of modulation is given by $F_{ij} = \Delta f_{ij} \sum \delta(2\pi(\mathbf{Q} + \mathbf{q}) - \mathbf{G}_{hkl})$, where $\mathbf{G}_{hkl}$ is a generic reciprocal-lattice vector. Thus, each term of the structure factor tensor is equal to the amplitude of the atomic Δf_{ij} modulation.

The AAST in the hard-x-ray region depends on the local structure around the scattered atom [5,7]. Any change in the

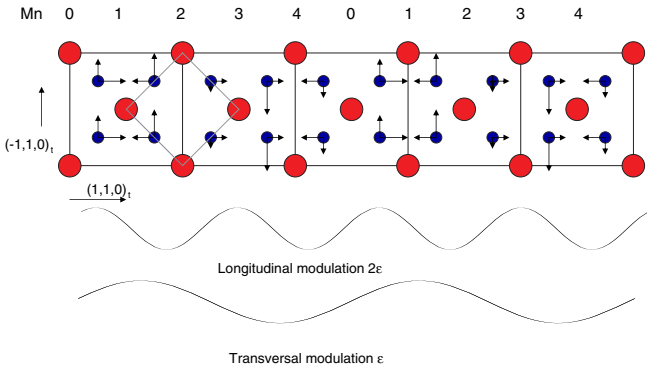

FIG. 2 (color online). Schematic picture in the $\mathbf{a}_o$-$\mathbf{b}_o$ plane of the proposed sinusoidal oxygen modulations in the low-temperature $La_{0.4}Sr_{1.6}MnO_4$ supercell. Longitudinal and transverse atomic displacements for the five nonequivalent MnO_6 octahedra with the central position $x = (5N + p)d^t_{110}$ (N: arbitrary integer, $p: 0, 1, 2, 3, 4$) are indicated by arrows. Only one of the two MnO_2 planes is shown for the sake of clarity. Big red circles represent Mn and small blue circles represent O atoms.

coordination geometry of the scattered atom is reflected on the AAST terms, and for small atomic displacements, the variation of the AAST is linear with the magnitude of the distortions. Here, the modulation of the atomic positions of the nearest-neighbor oxygen atoms will induce the same kind of modulation in the AAST terms of the Mn atoms that will be correlated to a modulation of the multipole terms of the local charge distribution. A uniform compression or expansion of the bond lengths will affect the diagonal components of the AAST (charge monopoles) whereas a deformation maintaining the average bond distances will act on the out of diagonal components (charge quadrupoles). Regarding our specific problem, $(h \pm 0.4\ h \pm 0.4\ 0)_t$ and $(h \pm 0.2\ h \pm 0.2\ 0)_t$ reflections correspond to a uniform and an anisotropic modulation of the interatomic distances, respectively.

Now, we check the sinusoidal modulation in a particular case (α is fixed). The value of α is chosen so as to reproduce the checkerboard ordering of the Mn atoms in $La_{0.5}Sr_{1.5}MnO_4$. The sinusoidal modulation will follow the $\mathbf{a_o}$ axis in the orthorhombic cell $\sqrt{2}\mathbf{a}_t \times \sqrt{2}\mathbf{a}_t \times \mathbf{c}_t$. RXS of the half-doped manganite is well described as due to the distortion originated by the three soft modes: $\Delta_2(B_{2u})$, $X_1^+(B_{2u})$, and $X_1^+(A)$ [8]. In the present case, only a longitudinal modulation of the oxygen atoms in the $\mathbf{a}_o$-$\mathbf{b}_o$ plane, given by $\Delta x = \Delta x_0 \cos(2\pi \times n \times 2\varepsilon)$, is present for the $X_1^+(B_{2u})$ monopole mode. The same type of modulation is considered for the $X_1^+(A)$ mode acting on the apical oxygen atoms (along the $\mathbf{c_o}$ axis). Finally, the transverse modulation for the $\Delta_2(B_{2u})$ quadrupole mode follows the expression, $\Delta y = \Delta y_0[\cos(2\pi \times n \times \varepsilon) + \sin(2\pi \times n \times \varepsilon)]$. The same movements yield a checkerboard sequence of an expanded-distorted and compressed-undistorted MnO_6 octahedron for $2\varepsilon = 0.5$.

We show this superstructure model for $2\varepsilon = 0.4$ in Fig. 2, which is commensurate with five cells in the $\mathbf{a}_o$ direction. We can identify five different Mn sites resulting from the above modulations of the oxygen atoms. The AAST for each of the five distinct Mn atoms were calculated for a cluster radius of about 5 Å using the program FDMNES [24]. We have got that the only elements of the AAST, which give nonzero contributions are the diagonal f_{xx}, f_{yy}, and f_{zz} components and the off-diagonal element f_{xy}. We have then calculated the anomalous structure factor tensor for reflections of the $(h'00)$-type corresponding to the $(h/10\ h/10\ 0)_t$-type using tetragonal Miller indices. Only $((h'00)$ reflections with h' even have a nonzero structure factor. Therefore, the structure factor for the $((10(h \pm 0.4)00)$ reflections is $F(10(h \pm 0.4)00) = \Delta F_{yy}\cos^2\varphi + \Delta F_{zz}\sin^2\varphi$ in the σ-σ' channel, whereas the structure factor of the $(10(h \pm 0.2)00)$ reflections in the σ-π' channel will mainly follow the modulation of the F_{xy} term and it is given by $F(10(h \pm 0.2)00) = \Delta F_{xy}\cos\theta\cos\varphi$. This formulation accounts for the observed azimuthal behavior: Similar ΔF_{yy} and ΔF_{zz} amplitudes barely produce any significant intensity variation of $(10(h \pm 0.4)00)$ reflections as a function of φ, whereas ATS $(10(h \pm 0.2)00)$ reflections show a pronounced $\cos^2\varphi$ dependence as experimentally observed.

Figure 3 compares calculated and experimental spectra for representative reflections of $La_{0.4}Sr_{1.6}MnO_4$ and the half-doped sample. We obtained a satisfactory agreement with the values of the refined distortions for the longitudinal, transverse, and apical modulations: $\Delta x_0 = 0.002$ Å, $\Delta y_0 = 0.014$ Å, and $\Delta z_0 = 0.001$ Å, respectively. The amplitude of the oxygen displacements for any of the modulations is significantly smaller than that found in $La_{0.5}Sr_{1.5}MnO_4$ ($\Delta x_0 = 0.02$ Å, $\Delta y_0 = 0.07$ Å, and $\Delta z_0 = 0.008$ Å), indicating that the oxygen displacements decrease with the hole doping. In the case of superlattice $(10(h \pm 0.4)00)$ reflections, ΔF_{yy} and ΔF_{zz} can be related to the chemical shift arising from a charge disproportionation among the different Mn atoms in the unit cell due to the sinusoidal modulation. We obtain that the maximum chemical shift is about 0.1 eV. This corresponds to a charge disproportionation of ± 0.03 electrons.

This study demonstrates that the occurrence of $(h \pm 0.4\ h \pm 0.4\ 0)_t$ and $(h \pm 0.2\ h \pm 0.2\ 0)_t$ reflections is originated by sinusoidal oxygen motions, longitudinal and transverse to the modulation direction (orthorhombic $\mathbf{a}_o$ vector). Reflections that arise from the transverse modulation in the a_o-b_o plane are forbidden for Thomson scattering and they are only detected in the σ-π' polarization channel. On the other hand, characteristic reflections of the longitudinal modulation show Thomson scattering and the resonance at $\varphi = 0°$ is σ-σ' polarized. The apical motion gives a contribution to this σ-σ' resonance at $\varphi = 90°$. Thus, our RXS results confirm that the two modulations with $\varepsilon = 0.2$ and $2\varepsilon = 0.4$ have a different origin, i.e., the modulation with $2\varepsilon = 0.4$ does not correspond to the second harmonic of the modulation with $\varepsilon = 0.2$. In

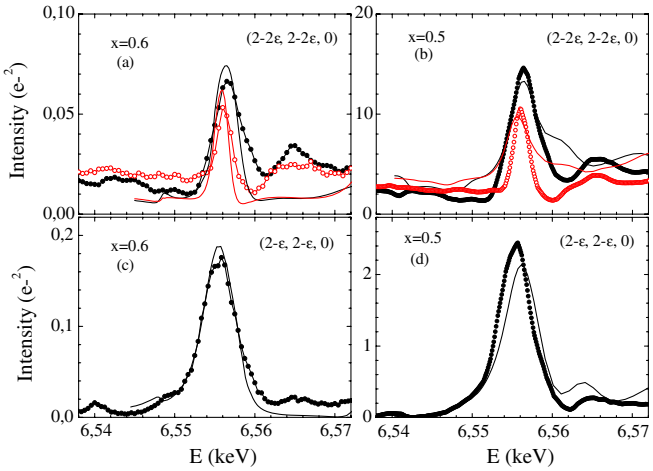

FIG. 3 (color online). Energy dependence of the FDMNES calculated and experimental intensities for $La_{1-x}Sr_{1+x}MnO_4$ ($x = 0.5$ and 0.6) of (a), (b) the $(2-2\varepsilon\ 2-2\varepsilon\ 0)_t$ superlattice reflections collected in the σ-σ' polarization channel. Closed and open symbols are the experimental spectra at $\varphi = 0°$ and $\varphi = 90°$, respectively. Solid lines are the best-fit calculations and (c) and (d) are the $(2-\varepsilon\ 2-\varepsilon\ 0)_t$ ATS reflections collected in the σ-π' polarization channel. Symbols are the experimental spectra at $\varphi = 0°$ and lines are the best-fit calculations.

conclusion, we have solved a long controversy between the two proposed models, i.e., charge stripes vs continuous charge-orbital density waves, to describe the low-temperature incommensurate-ordered phases in overdoped manganites. Our results clearly confirm the existence of a charge-density-wave ordering [27]. The continuous change of the periodicity with either the doping [16,17] or the temperature [18] agrees with a continuous variation of the oxygen structural modulations. The origin of the semiconductor-insulator phase transition would then be explained by a Peierls opening of a gap with a periodicity that involves a superlattice cell containing an integer number of e_g electrons. The lack of charge stripes in layered manganites has profound implications in the physics of other doped Mott insulators such as cuprates, nickelates, and cobaltates, where stripes were also proposed [28–30].

The authors thank ESRF for granting beam time. Financial support from the Spanish MICINN (project FIS08-03951 and MAT2007-61621) and DGA (CAMRADS) is acknowledged. J. H.-M. thanks CSIC for the JAEdoc contract, which is cofinanced by the European Social Fund.

*Author to whom correspondence should be addressed.
jgr@unizar.es

[1] Y. Moritomo, Y. Tomioka, A. Asamitsu, Y. Tokura, and Y. Matsui, Phys. Rev. B **51**, 3297 (1995).
[2] P. G. Radaelli, D. E. Cox, M. Marezio, and S.-W. Cheong, Phys. Rev. B **55**, 3015 (1997).
[3] S. Mori, C. H. Chen, and S.-W. Cheong, Nature (London) **392**, 473 (1998).
[4] Y. Murakami, H. Kawada, H. Kawata, M. Tanaka, T. Arima, Y. Moritomo, and Y. Tokura, Phys. Rev. Lett. **80**, 1932 (1998).
[5] J. Herrero-Martín, J. García, G. Subías, J. Blasco, and M. C. Sánchez, Phys. Rev. B **70**, 024408 (2004).
[6] S. Grenier *et al.*, Phys. Rev. B **69**, 134419 (2004).
[7] G. Subías, J. García, P. Beran, M. Nevřiva, M. C. Sánchez, and J. L. García-Muñoz, Phys. Rev. B **73**, 205107 (2006).
[8] J. Herrero-Martín, J. Blasco, J. García, G. Subías, and C. Mazzoli, Phys. Rev. B **83**, 184101 (2011).
[9] C. H. Chen, S.-W. Cheong, and H. Y. Hwang, J. Appl. Phys. **81**, 4326 (1997).
[10] P. G. Radaelli, D. E. Cox, L. Capogna, S.-W. Cheong, and M. Marezio, Phys. Rev. B **59**, 14440 (1999).
[11] J. Wang, J. Gui, Y. Zhu, and A. R. Moodenbaugh, Phys. Rev. B **61**, 11946 (2000).
[12] H. Ulbrich, D. Senff, P. Steffens, O. J. Schumann, Y. Sidis, P. Reutler, A. Revcolevschi, and M. Braden, Phys. Rev. Lett. **106**, 157201 (2011).
[13] T. Kimura, K. Hatsuda, Y. Ueno, R. Kajimoto, H. Mochizuki, H. Yoshizawa, T. Nagai, Y. Matsui, A. Yamazaki, and Y. Tokura, Phys. Rev. B **65**, 020407 (2001).
[14] L. Brey, Phys. Rev. Lett. **92**, 127202 (2004).
[15] G. C. Milward, M. J. Calderon, and Littlewood, Nature (London) **433**, 607 (2005).
[16] S. Larochelle, A. Mehta, N. Kaneko, P. K. Mang, A. F. Panchula, L. Zhou, J. Arthur, and M. Greven, Phys. Rev. Lett. **87**, 095502 (2001).
[17] S. Larochelle, A. Mehta, L. Lu, P. K. Mang, O. P. Vajk, N. Kaneko, J. W. Lynn, L. Zhou, and M. Greven, Phys. Rev. B **71**, 024435 (2005).
[18] J. C. Loudon, S. Cox, A. J. Williams, J. P. Attfield, P. B. Littlewood, P. A. Midgley, and N. D. Mathur, Phys. Rev. Lett. **94**, 097202 (2005).
[19] T. Nagai, T. Kimura, A. Yamazaki, Y. Tomioka, K. Kimoto, Y. Tokura, and Y. Matsui, Phys. Rev. B **68**, 092405 (2003).
[20] A. Nucara, P. Maselli, P. Calvani, R. Sopracase, M. Ortolani, G. Gruener, M. Cestelli Guidi, U. Schade, and J. García, Phys. Rev. Lett. **101**, 066407 (2008).
[21] M. Arao, Y. Inoue, K. Toyoda, and Y. Koyama, Phys. Rev. B **84**, 014102 (2011).
[22] J. Blasco, M. C. Sánchez, J. García, J. Stankiewicz, and J. Herrero-Martín, J. Cryst. Growth **310**, 3247 (2008).
[23] L. Paolasini *et al.*, J. Synchrotron Radiat. **14**, 301 (2007).
[24] Y. Yoly, Phys. Rev. B **63**, 125120 (2001).
[25] *Resonant Anomalous X-ray Scattering*, edited by G. Materlick, C. Sparks, and K. Fischer (North Holland, Amsterdam, 1994).
[26] V. E. Dmitrienko, K. Ishida, A. Kirfel, and E. N. Ovchinnikova, Acta Crystallogr. Sect. A **61**, 481 (2005).
[27] G. Grüner, Rev. Mod. Phys. **60**, 1129 (1988).
[28] J. M. Tranquada, B. J. Sternlieb, J. D. Axe, Y. Nakamura, and S. Uchida, Nature (London) **375**, 561 (1995).
[29] J. M. Tranquada, D. J. Buttrey, and V. Sachan, Phys. Rev. B **54**, 12318 (1996).
[30] M. Cwik, M. Benomar, T. Finger, Y. Sidis, D. Senff, M. Reuther, T. Lorenz, and M. Braden, Phys. Rev. Lett. **102**, 057201 (2009).